Paweł FEDOROWICZ, Ireneusz URBANIEC, Sławomir KRZEWIŃSKI
OPOLE UNIVERSITY OF TECHNOLOGY, FACULTY OF ELECTRICAL ENGINEERING, AUTOMATIC CONTROL AND INFORMATICS
Gen. K. Sosnkowskiego 31, 45-272 Opole

Analysis of optical signals emitted by SPD on an insulator model

M.Sc. Paweł FEDOROWICZ

He received the M.Sc. degree in Electrical Engineer- from the Faculty of Electrical Engineering, Automatics and Informatics at Opole University of Technology, Poland. His research interests include high voltage technique, optical metrology and artificial intelligence systems.

e-mail: pawel_fedorowicz@tlen.pl

M.Sc. Ireneusz URBANIEC

He received the M.Sc. degree in Electrical Engineer- from the Faculty of Electrical Engineering, Automatics and Informatics at Opole University of Technology, Poland. His research interests include optical emission phenomena connected with electrical discharges.

e-mail: i.urbaniec@interia.pl

M.Sc. Sławomir KRZEWIŃSKI

He received the M.Sc. degree in Electrical Engineer- from the Faculty of Electrical Engineering, Automatics and Informatics at Opole University of Technology, Poland. He is studying emission spectra of corona discharges occurring on power transmission lines.

e-mail: sławomir.krzewinski@radio.opole.pl

Abstract

The paper presents the analysis results of optical signals measured by photographic technique. The optical signals were emitted by surface discharges occurring on two models of bushing and two models of post insulators during tests under laboratory conditions. The analyses were carried out in order to determine the impact of changes in distance between the HV source and the grounding on the intensity of emitted optical radiation according to red, green and blue components. In addition, the influence of discharge duration on the optical emission intensity was estimated.

Keywords: photographic technique, surface discharges, bushing, support/post insulator.

Analiza sygnałów optycznych emitowanych przez WNZ powierzchniowe na modelu izolatora

Streszczenie

W artykule przedstawiono wyniki analizy sygnałów optycznych mierzonych techniką fotograficzną. Sygnały optyczne emitowane były przez wyładowania niezupełne typu powierzchniowego, występujące na dwóch modelach izolatora przepustowego i na dwóch modelach izolatora wsporczego. Pomiary wykonano w warunkach laboratoryjnych. Analizy przeprowadzono w celu określenia wpływu zmiany odległości między źródłem wysokiego napięcia i uziemieniem na intensywność emitowanego promieniowania optycznego w zakresie barw czerwonej, zielonej i niebieskiej. Ponadto określono wpływ na intensywność emisji optycznej czasu trwania wyładowań. W pierwszej sekcji naświetlono problematykę zagadnienia oraz odwołano się do 10 prac dotyczących omawianej tematyki. W sekcji drugiej krótko scharakteryzowano izolatory wsporcze i przepustowe. W sekcji trzeciej opisano modele badanych izolatorów, zawarto trzy schematy blokowe oraz opisano metodologię pomiaru. W sekcji czwartej zawarto równania matematyczne wykorzystane do obliczenia intensywności składowych RGB zarejestrowanego promieniowania optycznego oraz osiem rysunków prezentujących wyniki przeprowadzonych analiz. W sekcji piątej szczegółowo omówiono otrzymane wyniki oraz zamieszczono podsumowanie uzyskanych charakterystyk.

Słowa kluczowe: technika fotograficzna, wyładowania powierzchniowe, izolator przepustowy, izolator wsporczy.

1. Introduction

One of the problems of insulation systems used in electrical equipment and high voltage transmission lines is worsening of insulating properties induced by progressing of the aging process. Reduction of aging resistance is caused by a number of external factors, which may include exposure to atmospheric, environmental and voltage. Important aging factors that occur during service practice include UV radiation, the presence of ozone and oxides of nitrogen, temperature fluctuations, rain (also acid rain), and deposition of hoar frost, dirt and partial discharges (PD) [1]. Rainfalls have relatively low hazardous and are a so far less explored aging exposure factor of insulators, especially such made from composite. They may lead to loss of hydrophobicity of insulator and thus to an increase in the leakage current and development of surface discharges (SPD). Impurities that accumulate on the surface of high voltage insulators cause a decrease in their insulating capacity. The occurrences of contaminants, as well as high levels of humidity are the cause of formation of conductive paths, which are the source of PD [2]. The quantity, amplitude and intensity of PD, which may be generated in high-voltage electrical equipment, are the critical values in the evaluation and determining the quality of insulation. Their presence may have a direct impact on the stability and proper operation of the power system, because they may contribute to the emergence of failure and in extreme cases cause a breakdown in the power supply. Diagnostic techniques are most commonly used to monitor values of selected parameters, which if critical, may inform about the possibility of breakdown or permanent damage to the considered entity. In recent years, there has been a rapid development of various techniques for monitoring, analyzing and evaluating the work of electrical equipment, which are now an integral part of the electricity production, transmission and distribution systems [3]. In addition to conventional methods for PD measuring, which are defined in the IEC 60270 standard: HF/VHF/UHF electrical methods, alternative nondestructive approaches are increasingly being used in the diagnosis of insulation systems [4, 5, 6]. They include optical, acoustic and chemicals methods. Electrical methods are mainly used to detect and quantify the discharges. However, acoustic methods apart from detection allow also for localization of PD. In practical diagnostic applications one also applies measurement methods for radio interference tension, thermograph and visual observations [7]. The phenomena of temperature increase in the vicinity of PD occurrence in gas facilities are described among others in [8]. In [9] the authors state that the most effective determination of the condition of the insulation is achieved by a combination of several methods and pattern recognition techniques. Measurement possibilities of PD occurring in high voltage devices and insulation used in diagnostics and some examples of measurement systems using different diagnostic methods is described, among others in [10].

The main aim of the authors was to identify the extent of such a wavelength of recorded optical radiation in the range from 270 nm to 1700 nm, for which the intensity would have the largest and stable value, and would not be influenced by interfering external factors. For this purpose, measurements of optical radiation emitted by SPD generated on two systems modeling bushing and support (post) insulators were performed by the use of photographic technique. A camera recorded three color components: blue with wavelength from about 420 to about 490 nm, green with wavelength of about 550 nm and red with wavelength from about 630 to about 780 nm. In particular, this paper presents the analysis results of the impact of changes in distance between the HV source and the grounding on the intensity of emitted optical radiation according to the red, green and blue component. Furthermore, the effect of SPD generation duration on the optical radiation intensity, which was conducted separately for the red, green and blue components, is shown.

A short characteristic of the support (post) and bushings insulators is included in Section 2. Two models of insulators, used in research works and the experiment methodology are described in Section 3. In Section 4 the analysis results are presented and then discussed in the final Section 5.

2. Characteristics of bushing and post insulators

From the viewpoint of distribution of electric fields, the bushing and post insulators are two basic solutions, which have practical application in the isolation technique. Insulators are devices that are used in electrical power engineering for supporting, mechanical joining, mounting and insulating of electrical circuits components, mostly electrical equipment or wiring between which there is a potential difference. They are classified as outer insulation, because their electrical resistance usually determines the value of voltage breakdown in the air.

The post insulator is designed for rigid supporting of the conductive portion, which is to be insulated from the ground or from another part, which is under voltage. It supports current paths or hoods connected to other insulators, thus creating an insulation column. Moreover, it is used for mounting the contacts and fuses in switches and disconnections. Post insulators are not exposed to significant mechanical stresses during their normal operation. However, they must withstand some defined dynamic pressures induced by flow of short-circuit currents. The post insulator is a classic and one of the simplest example of a parallel layered system, wherein the electric field intensity has the same value on both sides of the surface border in each of the dielectrics. By identical electrical field strengths the flashover arc occurs in dielectric with a lower strength. Equivalent circuits of this type systems, in particular for long rod and cap-chain insulators, the equations describing the physics of the analyzed phenomena and graphs showing the dependence of the breakdown voltage on the distance between the electrodes, have been widely discussed in the literature, among others in [7, 9].

A bushing insulator is a construction allowing for carrying out by wall or partition, or in distribution stations, through reservoirs and grounded transformer covers, capacitors, generators, shunt transformers and switches of one or several conductors, and for isolating them from the partition. Wherein the mounting (flange or clamping device) to the partition is a part of the bushing. In the most general way bushing insulators can be divided into station and apparatus. Depending on the application, operating conditions, and function there are outdoor, indoor and outdoor-oil insulators. Bushing is a classical example of a diagonally layered system. Voltage distribution in such an insulator depends mainly on the surface capacity and the capacity of the dielectric sandwiched between electrodes.

3. Models of insulators and experiment methodology

For the generation of SPD on the surface of bushing and post insulators two models for each type were developed and constructed. Schematic representations of these models are shown in Fig. 1. Both models are made from porcelain. In the case of bushing (BUSH) and post (POST) insulators model I, factory fresh transformer oil was filled into eight openings, which are arranged along the entire length of the device. Each of the symmetrically arranged openings has a diameter of 0.7 cm (see Fig. 2). Furthermore, both constructions differ in geometric size, i.e. the diameter equals 5 cm in model I and 6 cm in model II; the height equals 34 cm in model I and 44 cm in model II. The bushing insulators of both constructions were designed in the way that an aluminum inlay of a diameter equal to $d = 9.9$ mm was moved into the opening in the center. The considered insulator models were supplied from a testing system allowing for continuous adjustment of the applied HV in the range from 0 to 60 kV. Measurements were made by supplying a voltage value equal to 0.99 Up on the movable clamp, while the distance between the HV source and the grounding was changed for each recording in 1 cm intervals from 1 to 24 cm. For the measurements a four-channel Acquitek data acquisition card type CH3160, equipped with a SDK library, was used. The measuring card has a resolution of 12 bit and allows for sampling rates up to 40 MHz. It has seven input ranges: ± 50 mV, ± 100 mV, ± 200 mV, ± 500 mV, ± 1 V, ± 2 V, ± 5 V. During the measurements we used two of them, i.e. 100 and 200 mV. The input impedance is adjustable and may be selected between 1 MW and 50 Ω.

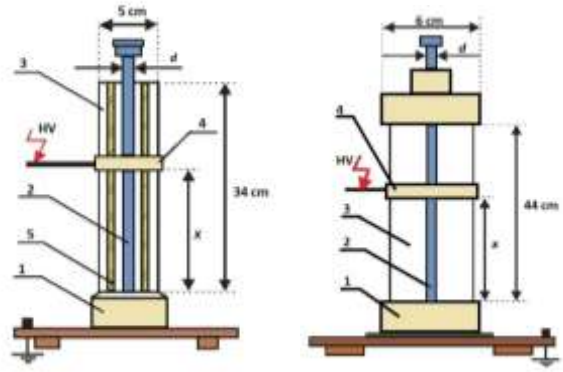

Fig. 1. Schematic diagram of the post and bushing insulators: left – model I, right – model II, where: 1- grounded ferrule, 2 – opening for aluminum inlay for bushing insulator design, 3- ceramic insulation, 4- movable clamp, 5- transformer oil, X – distance between HV source and grounding, $d = 9.9$ mm

Rys. 1. Schemat ideowy układu modelującego izolator przepustowy i wsporczy: po lewej – model I, po prawej – model II, gdzie: 1- uziemione okucie, 2- otwór na metalowy wkład dla izolatora przepustowego, 3 – izolacja ceramiczna 4- ruchoma obejma, 5- olej transformatorowy, X – odległość między elektrodą HV a uziemieniem, $d = 9.9$ mm

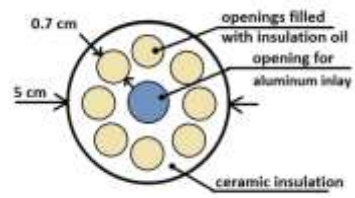

Fig. 2. Cross section of insulator model I

Rys. 2. Przekrój poprzeczny modelu izolatora I

The study was carried out using the photographic technique. To capture RGB images a Nikon D7000 (CMOS) camera was used. The camera shutter was triggered by an infrared transmitter. This transmitter was controlled by a microprocessor system, designed and implemented specially for this task. All measurements were performed by a constant temperature level equal to 17 ºC (± 0.5 ºC). The camera resolution used for the measurements was: X = 2464, Y = 1632. All the experiments were performed in a laboratory with curtained windows, which eliminated the entrance of the daylight. The distance between the camera lens and the movable clamp, where HV was applied to, was constant and equal to 2.7 m. All the images were taken using the same camera settings.

4. Analysis results

For calculation of the intensities of the R,G,B components I_R, I_G, I_B the following equations were applied:

$$I_R = \begin{cases} \frac{1}{XY}\sum_{x=1}^{X}\sum_{y=1}^{Y} R(x,y) & \text{for } R(x,y) > P_R \\ 0 & \text{for } R(x,y) \le P_R \end{cases} \quad (1)$$

$$I_G = \begin{cases} \frac{1}{XY}\sum_{x=1}^{X}\sum_{y=1}^{Y} G(x,y) & \text{for } G(x,y) > P_G \\ 0 & \text{for } G(x,y) \le P_G \end{cases} \quad (2)$$

$$I_B = \begin{cases} \frac{1}{XY}\sum_{x=1}^{X}\sum_{y=1}^{Y} B(x,y) & \text{for } B(x,y) > P_B \\ 0 & \text{for } B(x,y) \le P_B \end{cases} \quad (3)$$

For each R,G,B image matrix that presents the measurement results of particular constituents, discrimination thresholds: PR, PG, PB, that are necessary to reduce the noise in the used matrix were applied. The threshold values were calculated based on empirically estimated constants, arithmetic means and standard deviations of the measured R,G,B values as shown in Eq. (4)-(6).

$$P_R = 1.7 * mean(R) + 3 * std(R) \quad (4)$$

$$P_G = 2.0 * mean(G) + 3 * std(G) \quad (5)$$

$$P_B = 1.4 * mean(B) + 3 * std(B) \quad (6)$$

Figs. 3-6 show characteristics illustrating changes in the intensity values of three registered color components, assigned as a function of the distance between the electrodes (source of HV and the grounding), determined for the same relative value of the power supply voltage equal to 0.99 *Up*. Such a set of diagrams enable the comparative analysis of all the studied insulator systems, i.e. the bushing and post insulator model I – with insulation oil filled into the openings and the pure ceramic bushing and post insulators – model II.

In Figs. 7-10 histograms illustrating the distributions of probability densities calculated for the recorded intensities of optical radiation are shown. The optical signals were measured during 70 minutes period with 0.5 minute time intervals between each recording for POST II and for 30 minutes for the other insulator type. SPD were generated with the same relative value of the supply voltage equal to 0.99 *Up* and the same distance between the electrodes of 12 cm. The characteristics were determined separately for the red, green and blue components for all the four insulator models considered. For each of the histograms the standard deviation (σ) and the arithmetic mean (μ) were calculated and placed in the figures legends.

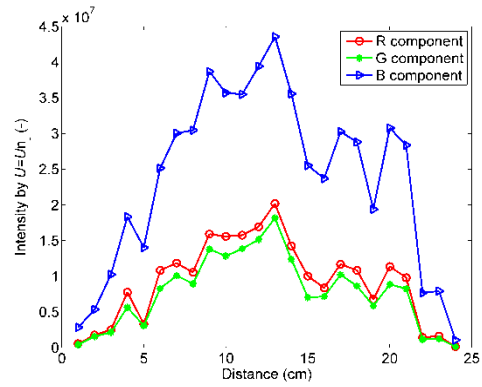

Fig. 3. Dependence of the intensity of optical radiation registered in the color ranges: red, green and blue, on the distance between the electrodes, while generating SPD at a voltage U = 0.99 *Up* on insulator model BUSH I

Rys. 3. Zależność intensywności promieniowania optycznego zarejestrowanego w zakresie barwy czerwonej, niebieskiej i zielonej w funkcji odległości między elektrodami, podczas generacji WNZ powierzchniowych przy napięciu U = 0,99 *Up* na modelu izolatora przepustowego model BUSH I

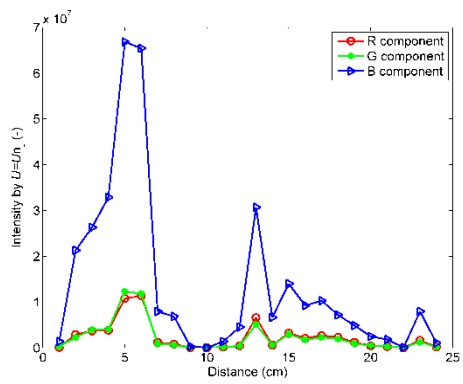

Fig. 4. Dependence of the intensity of optical radiation registered in the color ranges: red, green and blue, on the distance between the electrodes, while generating SPD at a voltage U = 0.99 *Up* on bushing insulator model BUSH II

Rys. 4. Zależność intensywności promieniowania optycznego zarejestrowanego w zakresie barwy czerwonej, niebieskiej i zielonej w funkcji odległości między elektrodami, podczas generacji WNZ powierzchniowych przy napięciu U = 0,99 *Up* na modelu izolatora przepustowego model BUSH II

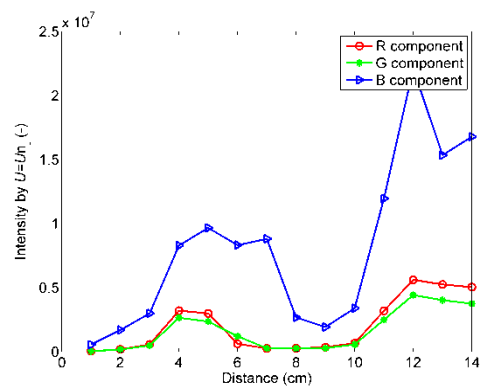

Fig. 5. Dependence of the intensity of optical radiation registered in the color ranges: red, green and blue, on the distance between the electrodes, while generating SPD at a voltage U = 0.99 *Up* on insulator model POST I

Rys. 5. Zależność intensywności promieniowania optycznego zarejestrowanego w zakresie barwy czerwonej, niebieskiej i zielonej w funkcji odległości między elektrodami, podczas generacji WNZ powierzchniowych przy napięciu U = 0,99 *Up* na modelu izolatora wsporczego model POST I

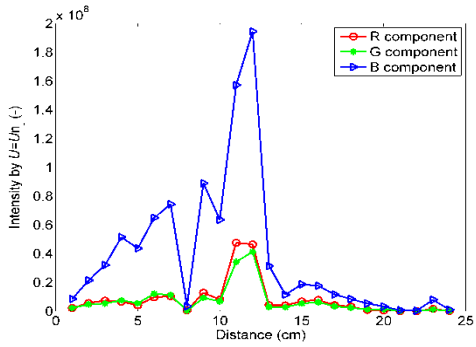

Fig. 6. Dependence of the intensity of optical radiation registered in the color ranges: red, green and blue, on the distance between the electrodes, while generating SPD at a voltage $U = 0.99\ Up$ on insulator model POST II

Rys. 6. Zależność intensywności promieniowania optycznego zarejestrowanego w zakresie barwy czerwonej, niebieskiej i zielonej w funkcji odległości między elektrodami, podczas generacji WNZ powierzchniowych przy napięciu $U = 0{,}99\ Up$ na modelu izolatora wsporczego model POST II

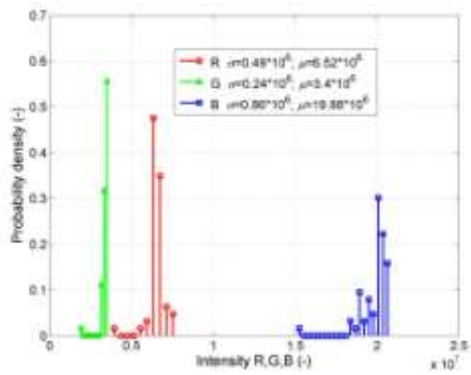

Fig. 7. Probability density distributions of optical radiation intensities calculated for color components: red, green and blue, emitted by SPD generated by a constant voltage equal to 0.99 *Up* and constant distance between electrodes equal to 12 cm, on the bushing insulator model BUSH I in a time duration of 30 minutes

Rys. 7. Rozkład gęstości prawdopodobieństwa intensywności promieniowania optycznego obliczone dla składowych barwy czerwonej, niebieskiej i zielonej, emitowanego przez WNZ powierzchniowe generowane przy stałym napięciu równym 0,99 *Up* i odległości między elektrodami równej 12 cm, dla izolatora przepustowego model BUSH I, w czasie równym 30 minut

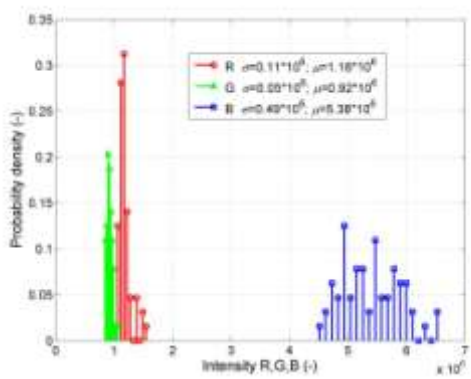

Fig. 8. Probability density distributions of optical radiation intensities calculated for color components: red, green and blue, emitted by SPD generated by a constant voltage equal to 0.99 *Up* and constant distance between electrodes equal to 12 cm, on the bushing insulator model BUSH II in a time duration of 30 minutes

Rys. 8. Rozkład gęstości prawdopodobieństwa intensywności promieniowania optycznego obliczone dla składowych barwy czerwonej, niebieskiej i zielonej, emitowanego przez WNZ powierzchniowe generowane przy stałym napięciu równym 0,99 *Up* i odległości między elektrodami równej 12 cm, dla izolatora przepustowego model BUSH II, w czasie równym 30 minut

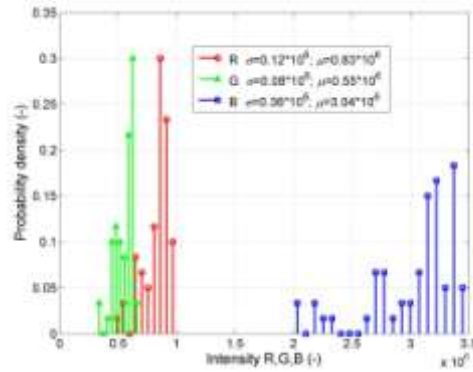

Fig. 9. Probability density distributions of optical radiation intensities calculated for color components: red, green and blue, emitted by SPD generated by a constant voltage equal to 0.99 *Up* and constant distance between electrodes equal to 12 cm, on the post insulator model POST I in a time duration of 30 minutes

Rys. 9. Rozkład gęstości prawdopodobieństwa intensywności promieniowania optycznego obliczone dla składowych barwy czerwonej, niebieskiej i zielonej, emitowanego przez WNZ powierzchniowe generowane przy stałym napięciu równym 0,99 *Up* i odległości między elektrodami równej 12 cm, dla izolatora wsporczego model POST I, w czasie równym 30 minut

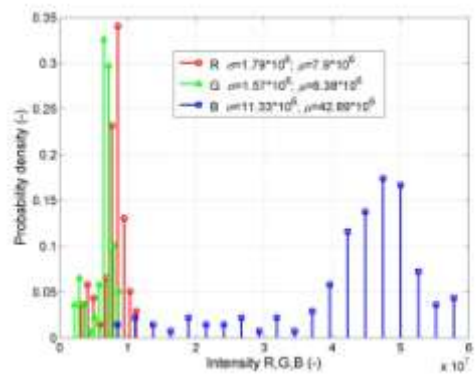

Fig. 10. Probability density distributions of optical radiation intensities calculated for color components: red, green and blue, emitted by SPD generated by a constant voltage equal to 0.99 *Up* and constant distance between electrodes equal to 12 cm, on the post insulator model POST II in a time duration of 70 minutes

Rys. 10. Rozkład gęstości prawdopodobieństwa intensywności promieniowania optycznego obliczone dla składowych barwy czerwonej, niebieskiej i zielonej, emitowanego przez WNZ powierzchniowe generowane przy stałym napięciu równym 0,99 *Up* i odległości między elektrodami równej 12 cm, dla izolatora wsporczego model POST II, w czasie równym 70 minut

5. Conclusions

Analyzing the nature of changes in the optical radiation at various distances between the electrodes, presented in Figs. 3-6, it can be seen that:

- For three of the studied models of insulators (POST I, BUSH II, POST II) a similar shape was obtained for the considered colors. The middle part of the porcelain insulation is characterized by a reduced radiation intensity of the blue and almost compete extinction of the red and green components. In particular, this regards to SPD generation at a distance between approximately 7 and 11 cm from the HV source to the grounding, for which the plotted charts achieve a local minimum, visible in the form of a saddle. This phenomenon is related to the formation of electric discharges that do not grow on the surface of the tested insulators, but cause a breakdown directly to the inner part of the porcelain. This is not the case for the bushing model I, which is probably due to the insulating nature of the transformer oil, which is filled into the openings.

- Characteristics obtained for the bushing insulator with oil filled into its openings (BUSH I) depict maximum R, G, B radiation intensity as discharges were generated in the central part of the test insulator. A decrease in the registered intensities occurs for the distances up to about 3 cm and above 21 cm. In these areas SPD generated far less energy and emitted less intense radiation. The estimated waveforms are similar to a bell curve.
- The extinguishing of SPD and the associated reduction of the registered optical radiation intensity can also be observed while considering the minimum and maximum distances, i.e.: 1 cm, 24 cm and 14 cm for the post insulator model I. However, for intermediate distances the intensity recorded for all three colors reaches the maximum value. On the presented charts there are two local maxima values in a form of characteristic peaks. For the system modeling the pure ceramic bushing insulator (model II) we observe greater radiation intensity values at the distance from 4 to 6 cm, as it is the case for the distances greater than 11 cm. However, for both post insulators (model I and II) and bushing model I, this relationship is reversed. For all the investigated insulators and for each color the calculated waveforms resemble with their shapes an unsymmetrical large letter M.

Based on the analyses performed, the results of which are shown in this paper, one can conclude that regardless of the insulator type (POST I, POST II, BUSH I, BUSH II) the highest radiation intensity was obtained for the blue component. Further, the red radiation intensity has a slightly higher value than the green radiation intensity, which was the lowest in all the gathered images. This relationship was confirmed by the probability density distributions shown in Figs. 7-10. From these charts one can also imply that in the entire experiment duration, which was equal to 30/70 minutes, while generating SPD at the distance between the electrodes equal to 12 cm, the smallest changes in the intensities were obtained for the red and green components. On the contrary, the blue color radiation is characterized by the most significant changes in its intensity.

6. References

[1] Kikuchi T., Nishimura S., Nagano M., Izumi K., Kubota Y., Sakata M.: Survey on the non-ceramic Composite Insulators, IEEE Transactions on DEI, vol. 6, no. 5, pp. 548-556, 1999.
[2] Li E.: The study of the characteristics of corona discharge, High Voltage Apparatus, vol. 6, pp. 16-21, 1998.
[3] Frącz P.: Influence estimation of the voltage value on the measurements results for the optical radiation generated by partial discharges on bushing isolator, Acta Physica Polonica. A, vol. 120, pp. 604-608, 2011.
[4] Wotzka D., Boczar T., Zmarzly D.: Analysis of acoustic wave propagation in a power transformer model, Acta Physica Polonica A, vol. 116, pp. 428-431, 2009.
[5] Boczar T., Zmarzły D.: The application of correlation analysis to acoustic emission pulses generated by partial discharges, Materials Evaluation, vol. 62, pp. 935-942, 2004.
[6] Cichoń A., Borucki S., Wotzka D.: Characteristics of acoustic emission signals generated by the contacts of the selector, Acta Physica Polonica A. vol. 122, pp. 804-807, 2012.
[7] Pinnangudi B., Gorur R., Kroese A.: Quantification of corona discharges on non-ceramic insulators, IEEE Transactions on DEI, vol. 12, no. 3, pp. 513-523, 2005.
[8] Baricos J., Dupuy J., Peyrous R., Schreiber G.: Corona discharge and energy transfer, Journal of Physics D: Applied Physics, vol. 11, pp. L187-L190, 1978.
[9] Morshuis P., Gulski E.: Diagnostic tools for condition monitoring of insulating materials, IEEE Annual Report Conf. on EI and Dielectric Phenomena, pp. 327-330, 1995.
[10] Cheng Y., Huang C., Li X.: Study of corona discharge pattern on high voltage transmission lines for inspecting faulty porcelain insulators, IEEE Transactions on Power Delivery, vol. 23, no. 2, pp. 945-952, 2008.

otrzymano / received: 07.02.2014
przyjęto do druku / accepted: 01.04.2014 *artykuł recenzowany / revised paper*

INFORMACJE

Nowa inicjatywa PAK

Na stronie internetowej Wydawnictwa PAK został utworzony dział: **Niepewność wyników pomiarów** w którym są zamieszczane aktualne informacje dotyczące problemów teoretycznych i praktycznych związanych z szacowaniem niepewności wyników pomiarów. W dziale znajdują się:

- aktualne informacje o publikacjach dotyczących niepewności wyników,
- informacje o przedsięwzięciach naukowo–technicznych i edukacyjnych, o tematyce związanej z niepewnością,
- dokumenty dotyczące niepewności,
- pytania do ekspertów (FAQs).

Zapraszamy:

- autorów opublikowanych prac dotyczących niepewności o nadsyłanie tekstów do zamieszczenia w tym dziale,
- organizatorów przedsięwzięć naukowo – technicznych lub edukacyjnych do nadsyłania informacji o imprezach planowanych lub odbytych,
- zainteresowanych zagadnieniami szczegółowymi do nadsyłania pytań do ekspertów.

Materiały mogą mieć formę plików lub linków do źródeł. Warunkiem zamieszczenia w tym dziale strony internetowej PAK materiałów lub linków jest przysłanie do redakcji PAK pocztą zwykłą zgody właściciela praw autorskich na takie rozpowszechnienie. Zamieszczanie i pobieranie materiałów i informacji w tym dziale strony internetowej jest bezpłatne. Redakcja PAK będzie nadzorować zawartość działu, ale za szczegółowe treści merytoryczne odpowiadają autorzy nadsyłanych materiałów.

Tadeusz SKUBIS
Redaktor naczelny Wydawnictwa PAK